NOTICE

CERTAIN DATA CONTAINED IN THIS DOCUMENT MAY BE DIFFICULT TO READ IN MICROFICHE PRODUCTS.

BNL-45393

Papers presented at the Symposium on
Detector Research and Development for
the Superconducting Super Collider,
Fort Worth, TX, October 15-18, 1990

A STUDY OF ELECTRO-OPTICAL MODULATORS FOR TRANSFER OF DETECTOR SIGNALS BY OPTICAL FIBERS*

T. Tsang, V. Radeka, T. Srinivasan-Rao, and W. J. Willis†

Brookhaven National Laboratory, Upton, NY 11973

†BNL and Columbia University, New York 10027

October 1990

*This research was supported by the U. S. Department of Energy:
Contract No. DE-AC02-76CH00016.

DISCLAIMER

BNL--45393

DE91 006349

A STUDY OF ELECTRO-OPTICAL MODULATORS FOR TRANSFER OF DETECTOR SIGNALS BY OPTICAL FIBERS

T. Tsang, V. Radeka, T. Srinivasan-Rao, and W. J. Willis*

Brookhaven National Laboratory, Upton, NY 11973
*BNL and Columbia University, New York, NY 10027

ABSTRACT

Preliminary results of an investigation to minimize the local electronics on the detector by the use of electro-optical intensity modulators are reported. The electrical signal from the detector is converted into an optical signal by a Mach-Zehnder interferometer modulator based on the properties of electro-optical crystals such as $LiNbO_3$. The modulator is driven by the electrical signal from a detector element such as the gas proportional straw tube. The optical signal is brought in from a remote source and exits on an optical fiber to a data collection site. The results of the first tests of optical modulators with respect to their application to particle detectors will be presented. These include the optical power requirement, the linearity, the dynamic range, and the noise characteristics. Finally, the outlook for their application on a large scale is discussed.

I. Introduction

In high energy particle accelerators such as the Superconducting Super Collider, the readout of detectors with 10^5 to 10^6 signal channels is recognized as a major challenge. This is particularly the case where the electron identification information has to be obtained at the trigger level, since it requires a high degree of parallelism in signal transfer and processing. Electron identification can be performed by transition radiation detectors and calorimeters. In this study, we address this challenge by using a novel concept of integrated electrooptic modulators and optical fiber "cables" to read all channels in parallel. The use of the optical modulator with high input impedance can relieve the power problem of electronic readout circuits, give more freedom in preamplifier design, and dramatically reduce the mass and volume of the output "cables", due to the lower mass and volume of the optical fibers compared to electrical cables. This technique is of particular importance for transition radiation detectors. In a cryogenic detector such as the liquid argon calorimeter this technique simplifies the cold feedthroughs and lowers the heat loss due to copper cables.

The novel concept will utilize a system of electrooptic modulators, fabricated on a single substrate, and powered by a remote CW operated 1.3 μm laser source. The light is brought in remotely on single-mode polarization preserving fibers and the optical output signal is carried on fibers. The principle of operation is based on the Mach-Zehnder optical interferometer. A schematic of this type of intensity modulator is shown in Figure 1. A polarized light beam travelling in a single transverse mode optical waveguide is split by refraction into two beams, carried a suitable distance and then rejoined, giving rise to interference. The interference is constructive when the two beams are in phase, and the full power exits to the output waveguide. If the lengths of the two arms differ by half of a wavelength (optical phase of π), the interference is destructive, and the optical power is radiated into the substrate.

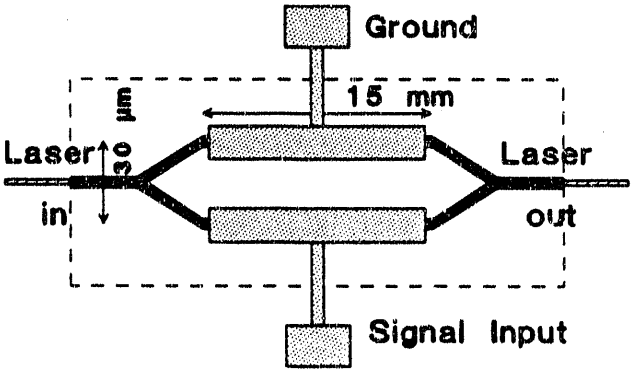

Figure 1. Mach-Zehnder Modulator

The single transverse mode optical waveguide is formed by Ti diffused into a planar $LiNbO_3$ substrate.

The principles of the device and the details of the state-of-the-art fabrication technology are given in review articles by Korotky [1] and Bulmer [2]. When a charge is injected on the electrode that is placed over one of the two arms of the electrooptic Ti : $LiNbO_3$ waveguides, the optical length of one arm becomes shorter than the other, changing the relative phase of the two beams at the end of the interferometer. The output power will then vary as the square of the cosine of the total phase shift, composed of a constant phase offset depending on the construction of the device, and a term due to the signal. The light signal then propagates on a low loss output fiber with very low time dispersion. The fiber can be one or more kilometers long, if a delay of that length is required. There it is received by a low noise semiconductor photodiode of high quantum efficiency and connected to a low noise preamplifier. The subsequent fast shaping and processing operations are done remote from the detector, so that the electronics on the detector can be minimized.

In this paper we intend to explore the operating parameters by studying a single modulator channel system first, and particularly, to examine closely the noise limitations, linearity, and the dynamic range.

II. Experimental Setup

The optical system comprises of a commercial diode-pumped Nd:YAG laser (Amoco), a Mach-Zehnder interferometric modulator (Crystal Technology) with x-cut y propagating Ti : $LiNbO_3$ electrooptic waveguides, low noise fast InGaAs photodiodes (Hamamatsu), low noise preamplifiers (BNL), and fast shaping amplifier (Ortec 579 and BNL). Figure 2 gives an overview of the experimental setup. The CW operated 1.3 μm infrared laser has a linearly polarized output with a power of 30 mW at the fiber output. It has a built-in 30 dB Faraday isolator, and a 50 meters long uncoated fiber pigtail. The output beam is recollimated and focused onto the optical fiber at the input end of the Mach-Zehnder modulator. The optical fiber ends were pigtailed to the input and the output ends of the waveguides. A half wave plate is employed to optimize the input polarization along the y-axis of the $LiNbO_3$ modulator to take advantage of the larger r_{33} electrooptic coefficient. A neutral density filter is used to adjust the optical power. After the output beam from the modulator is recollimated and focused onto the InGaAs photodiode, a neutral density filter is inserted until the photodiode achieved a photocurrent of $\sim$ 1 mA. Because the quantum efficiency of the InGaAs photodiode is 0.85 at 1.3 μm, this photocurrent corresponds to an incident laser power of 1.12 mW. The AC component of the photocurrent is then fed into a modified BNL IO-323 low noise preamplifier. The output of the preamplifier is then fed to an Ortec 579 fast timing filter amplifier which has integration and differentation times set at 20 ns. For faster pulse shaping time of $\sim$ 3 ns, a hybrid type filter amplifier made at BNL is employed. The data are collected on a 300 MHz Tektronic 2440 digital oscilloscope and stored on a computer for further analysis.

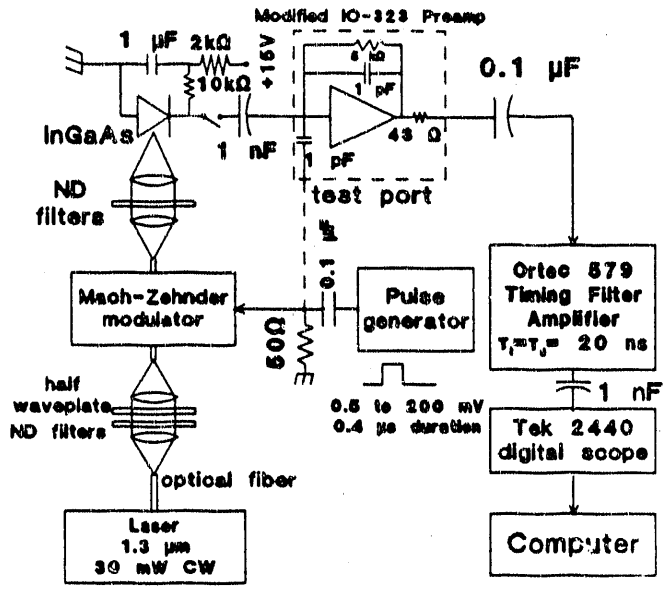

Figure 2. Experimental setup for noise measurements

The signal source used to investigate the transfer characteristics of the modulator is a $\pm$10 V ramp. To study the noise and the linearity of the modulated signal at the 20 ns shaping time, a voltage pulse with 6 ns risetime from a HP 8116A function generator is employed. For faster shaping time, a BNL pulser, BNL I0-391, with 2 ns risetime is used.

III. Results and Discussion

A. Transfer Characteristics

The particular Mach-Zehnder modulator employed has a -3 dB intensity modulation point close to the zero voltage bias point. The transfer characteristic is shown in Figure 3. The fringe intensity has an extinction ratio of 26 dB when the input polarization is optimized. The V_π voltage is 2.68 V. This low half wave voltage is achieved with an electrode length of 15 mm. An unoptimized input polarization of $\sim 2^\circ$ would shift up the visibility fringe pattern resulting in a change of the -3 dB intensity point by less than 0.01 dB. Therefore, the tolerance of the input polarization can be a few degrees.

B. Dynamic Range and Linearity

Given the output varying as the square of the cosine of the modulation voltage, the dynamic range will be determined by the requirement on linearity. In particle detector applications, two approaches are of interest. One is the case where a linear analog sum of many channels is needed, then linearity is required at some specified level in each channel in order to retain the accuracy of the sum. The other is where the nonlinear response is

well defined and the nonlinearity can be corrected. The modulator response is well defined and very large signals could be analyzed by observing the output signal over multiple fringes.

For operation in the quasi-linear regime the nonlinearity can be determined from the modulator response function. For a 1% maximum deviation from a tangent through the -3 dB point, the maximum signal is $\frac{0.25V_\pi}{\pi}$ or ~ 200 mV in our case. If the noise is limited by the photon statistics as discussed in the next section, the dynamic range with respect to the noise is given by,

$$\frac{v_{max}}{\sigma_{in}(v)} = \frac{Q_{max}}{\sigma_{in}(q)} = 0.25\sqrt{\frac{t_m n_o}{a_F}}, \qquad (1)$$

where n_o is the photoelectron rate at the detector, t_m is the integration time, and a_F is a filter parameter, usually in the range of $\frac{4}{3}$ to 2.

Assumming a light intensity at the detector of 1 mW, the photon rate is $n_o = 6.6 \times 10^{15}$ sec^{-1}. The integration time for our slower filter was $t_m = 35$ ns and $a_F = 1.9$. The expected dynamic range is then, $\frac{v_{max}}{\sigma_{in}(v)} = 2.7 \times 10^3$ All measurements were done with an input laser power of ~ 1 mW on the detection system. However, after all optical losses have been considered in our experimental setup, the optical power incident on the modulator is ~ 14 mW. The insertion loss of the modulator is ≤ 7 dB. Thus, the bias point is very important for the dynamic range.

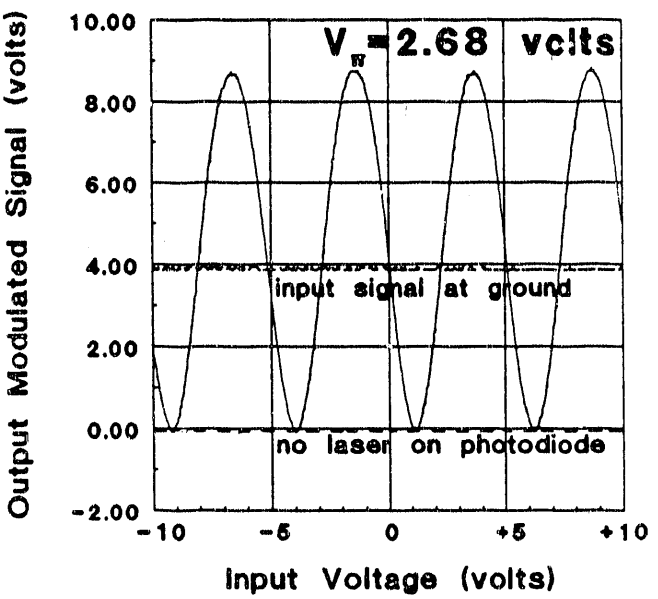

Figure 3. Transfer Characteristics

By measuring the voltage height of the modulator-receiver responses shown in Figure 4 with different input modulation voltages, a plot of the linearity curve is generated in Figure 5. The linearity of the modulated signal is quite good as expected, and the dynamic range approaches $3\frac{1}{2}$ decades. One possible improvement of the dynamic range is to operate the modulator at 0.2 V above or below the -3 dB point, but still in the linear regime, and inject an opposite polarity signal to the modulator.

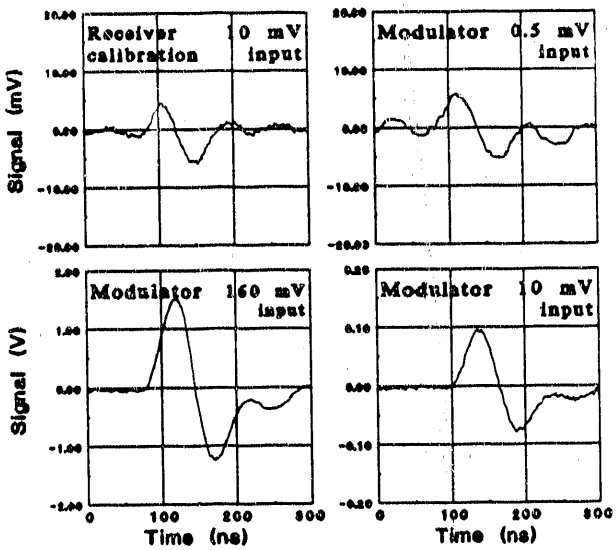

Figure 4. Modulator–Receiver Response at shaping time of $\tau_1=\tau_4=20$ ns (integration time $t_m=35$ ns) input equivalent noise $\sigma_{in}(v)=0.1$ mV

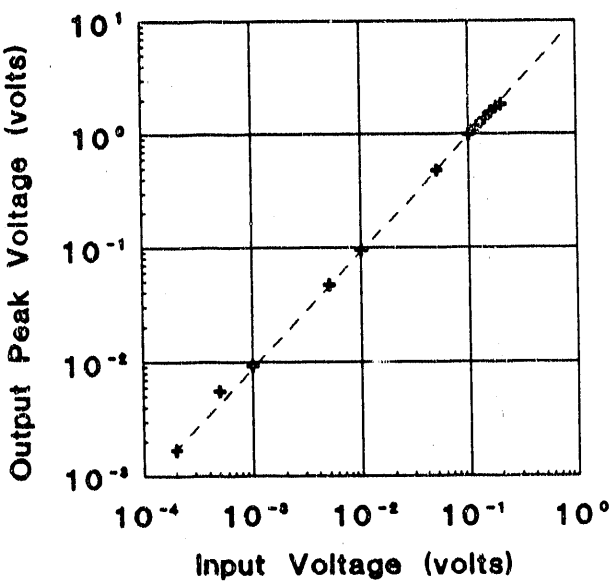

Figure 5. Linearity of the MZ Modulator

C. Noise Analysis

Five sources of noise may be considered in this experiment: (1) noise from the photodiode, (2) noise from the receiver system, (3) dielectric noise in the modulator (4) photon fluctations according to Poisson statistics, and (5) excess noise in the laser. We will discuss each of them individually in the following.

(1). Photodiodes

The Hamamatsu G3476-1 photodiode with infrared response has a junction capacitance of 0.8 pF and a measured dark current of $\sim$ 1nA at a reverse bias of 15V. In a measurement time of 20 to 40 ns (peaking time of the pulse shaper), this photocurrent corresponds to an rms noise of 200 electrons or less, which is much less than the photon noise that we would anticipate.

(2). Receiver-Detector System

The noise of the receiver-detector system includes the photodiode, the preamplifier and the pulse shaper, see Figure 2. Based on a calibration run of the system (see Figure 4), the receiver-detector system has a rms of $\leq 3 \times 10^3$ electrons ($\sim$ 0.5 fC), for t_m = 35 nsec, referred to the input of the receiver.

(3). Dielectric noise

The dielectric noise is that due to the thermal fluctuations in the dielectric constituting the modulator [3]. It can be evaluated from the dielectric loss factor for the$Ti : LiNbO_3$. Our estimate is that this will be less than 500 rms electrons, referred to the input of the modulator.

(4). Photon noise

The photoelectron statistics noise at the receiver is

$$\sigma(n) = \sqrt{a_F n_o t_m} , \qquad (2)$$

where a_F is the ratio of the effective measurement time for noise and the measurement time for the signal t_m. In the simplest case, the measurement is made on the modulator signal plus the baseline in one measurement interval, and in the other interval the baseline is measured and substracted from the first measurement. In this case $a_F = 2$. With pulse shaping of the signals from the receiver, lower values of a_F can be achieved (e.g., $a_F = \frac{4}{3}$ for a triangular bipolar shaping). The number of photoelectrons at the receiver produced during measurement time t_m by a step in the modulator input voltage is,

$$\Delta n\ t_m = \pi \frac{\Delta v_{in}}{V_\pi}\ t_m\ n_o , \qquad (3)$$

where Δn is the change in photoelectron rate caused by Δv_{in}. We obtain the equivalent input noise voltage from Eqs. (2) and (3) by substituting $\Delta n\ t_m = \sigma(n)$ and $\Delta v_{in} = \sigma_{in}(v)$,

$$\sigma_{in}(v) = \frac{V_\pi}{\pi} \sqrt{\frac{a_F}{t_m n_o}} . \qquad (4)$$

The equivalent input noise charge is,

$$\sigma_{in}(q) = (C_D + C_M)\, \sigma_{in}(v) ,$$

$$ENC_{in} = \sigma_{in}(q) = \frac{Q_\pi}{\pi} \left(1 + \frac{C_D}{C_M}\right) \sqrt{\frac{a_F}{t_m n_o}} , \qquad (5)$$

where $Q_\pi = C_M V_\pi$, C_M is the modulator electrode capacitance and C_D is the capacitance of the particle detector connected to the modulator. The parameter Q_π is independent of the modulator length ℓ, since $C_M \propto \ell$ and $V_\pi \propto 1/\ell$.

For 1.2 mW light input to the receiver diode, the average currrent is $I_o \simeq 1.07$ mA, and $n_o \simeq 6.7 \times 10^{15}$ sec^{-1}. For t_m = 35 ns, $a_F = 1.9$, the equivalent input noise voltage is $\sigma_{in}(v) = 84\ \mu$V. For $C_D \simeq C_M = 10$ pF, the equivalent noise charge is $\sigma_{in}(q) = 1.68$ fC. The noise at the receiver input is obtained from Eq. (2), $\sigma(n) = 2.05 \times 10^4$ e$^-$. The noise of the photon statistics is clearly dominant over other noise sources. With a step signal of 10 mV at the modulator input, and charge calibration of the receiver, we measured a signal of 1.28×10^6 e$^-$ and a signal to noise ratio of 57. This gives a noise of 2.25×10^4 rms electrons, which is about 11% higher than the calculated value. This difference is within the experimental accuracy of the noise measurement. To obtain a faster shaping time, a BNL made 2 ns risetime pulser and a hybrid circuit fast preamp and shaper with 3 ns peaking (integration) time were employed in the receiver-detector system. With 20 mV pulse input to the modulator, the response of this fast detection system is shown in Figure 6. Signal to noise ratio of 100 is obtained with an rms noise of $\sim 4 \times 10^3$ electrons at the receiver. The expected dynamic range with this integration time is 7×10^2

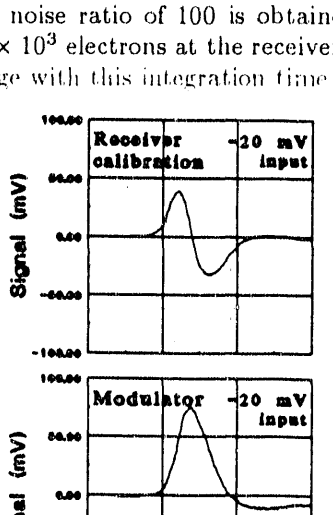

Figure 6. Modulator–Receiver Reponse at peaking time of t_m=3 ns

(5). Laser Excess Noise

Laser noise above the photon statistics was observed in the frequency range of 150-200 kHz. However this noise is not measureable after the pulse shaping filters used in our test.

IV. Application of Modulators for Transfer of Detector Signals

We are interested in two kinds of applications of modulators to particle detectors. One is where a low

noise preamplifier is used, and the other is without any preamplifier when the detector is connected directly to the modulator. In the first case the low capacitance and high sensitivity of the modulator allow much lower power dissipation in the preamplifier than with electrical cables. In the case of a modulator replacing a preamplifier, sufficiently low noise is obtained for some applications. For low capacitance detectors ($C_D \simeq 10$ pF), such as gas proportional tubes of up to 1 meter length, the noise will be in the range of $\approx$2 fC at $t_m \approx 35$ μsec. The equivalent noise charge (shown in Eq. (5)) is inversely proportional to the square root of the measurement time and the photon rate (laser power).

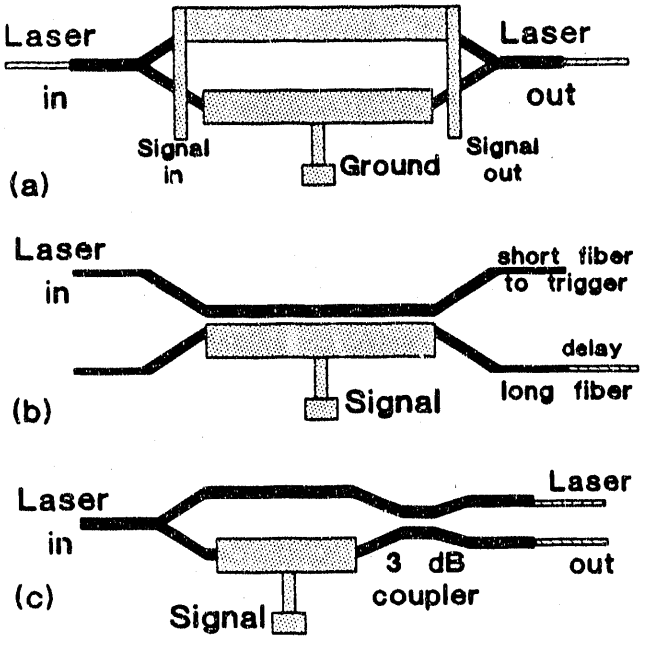

Figure 7. Schematics of (a) Mach-Zehnder type device (b) directional, and (c) 1x2 Y-junction couplers

Transfer of detector signals can be done in principle with various schemes using fiber optics communication technology [4]. Mach-Zehnder type device, 2×2 directional coupling, and 1 × 2 Y-junction splitting schemes (see Figure 7) have been used. In the last two schemes, a trigger signal can be obtained from the short fiber output of one signal arm while delaying the long fiber arm, to $1 - 5$ μs, for data collection. This scheme is particularly interesting because, one can perform some electronic processing or discrimination before storing the data. Finally, we should mention that there are several issues that are critical in realizing such a state-of-the-art detector. They are (a) the achievement of the optical power splitting among the channels on the device with adequate uniformity, (b) stability of the intrinsic and extrinsic bias point, (c) design and optimization of a full size modulator detector, (d) reliability of the fiber connectors, (e) power dissipation, (f) operation at low temperature, and (g) radiation damage to the modulators. These issues will be investigated in the next phase of this work.

Acknowledgements

We would like to acknowledge fruitful discussions with Drs. Steven Korotky of the AT&T and Catherine Bulmer of the Naval Research Laboratory. We appreciate the expert technical assistance of John Schill and Dmitri Stephani, and Barbara Kponou for the assistance with the manuscript.

This work has been supported under contract number DE-AC02-76CH00016 with the U.S. Department of Energy. Accordingly, the U.S. Government retains a nonexclusive, royalty-free license to publish or reproduce the published form of this contribution, or allow others to do so, for U.S. Government purposes.

References

1. S. K. Korotky and R. C. Alferness, *Optical Fiber Telecommunication II*, New York, Academic Press, Inc., 1988, ch. 11, pp. 421-465.
2. C. K. Bulmer and W. K. Burns, "Linear Interferometric Modulators in Ti : $LiNbO_3$," J. of Lightwave Technology, **LT-2**, pp. 512-521.
3. V. Radeka, Ann. Rev. Nucl. Part. Sci. **38**, pp. 217-277, 1988.
4. L. Thylen, "Integrated Optics in $LiNbO_3$: Recent Developments in Devices for Telecommunications," J. of Lightwave Technology, **LT-6**, pp. 847-861, 1988.

END

DATE FILMED

01 / 30 / 91